Optics Letters

Solitons supported by intensity-dependent dispersion

Chun-Yan Lin,[1] Jen-Hsu Chang,[2] Gershon Kurizki,[3] and Ray-Kuang Lee[1,4,*]

[1]*Institute of Photonics Technologies, National Tsing Hua University, Hsinchu 300, Taiwan*
[2]*Graduate School of National Defense, National Defense University, Taoyuan City 335, Taiwan*
[3]*Department of Chemical Physics, Weizmann Institute of Science, Rehovot 7610001, Israel*
[4]*Physics Division, National Center for Theoretical Sciences, Hsinchu 300, Taiwan*
Corresponding author: rklee@ee.nthu.edu.tw

Soliton solutions are studied for paraxial wave propagation with intensity-dependent dispersion. Although the corresponding Lagrangian density has a singularity, analytical solutions, derived by the pseudo-potential method and the corresponding phase diagram, exhibit one- and two-humped solitons with almost perfect agreement to numerical solutions. The results obtained in this work reveal a hitherto unexplored area of soliton physics associated with nonlinear corrections to wave dispersion. © 2020 Optical Society of America

Chromatic dispersion is the dependence of the phase velocity of a wave on its frequency [1] or, equivalently, frequency dependence of the refractive index. Nonlinear corrections to the chromatic dispersion as a function of the wave intensity arise for various waves, such as shallow water waves [2,3], acoustic waves in micro-inhomogeneous media [4], or ultrafast coherent pulses in GaAs/AlGaAs quantum well waveguide structures [5]. In the context of photon–atom interactions, nonlinear dispersion effects may come about from the saturation of the atomic-level population [6], electromagnetically induced transparency (EIT) in a chain-Λ configuration [7], or nonlocal nonlinearity mediated by dipole–dipole interactions [8].

The interplay between refractive-index nonlinearity and linear dispersion effects in a medium is expected to give rise to solitary, undistorted wavepacket shapes over extended travel distances. However, soliton solutions of this kind are still unknown. Here, we search for soliton solutions in paraxial wave propagation along the axis ζ, with an intensity-dependent dispersion,

$$i\frac{\partial \psi}{\partial \zeta} = \beta_2(|\psi|^2)\frac{\partial^2 \psi(\zeta,\tau)}{\partial \tau^2}, \qquad (1)$$

where $\psi(\zeta,\tau)$ describes the envelope function of the wave, and $\beta_2(|\psi|^2)$ denotes the intensity-dependent dispersion due to the interaction beyond the single-dipole term.

We may perform a Taylor expansion of the nonlinear dispersion term and restrict ourselves to the lowest-order quadratic correction, whose strength is measured by the nonlinear coefficient b, i.e.,

$$i\frac{\partial \psi}{\partial \zeta} = \beta_2^0(-1 + b|\psi|^2)\frac{\partial^2 \psi}{\partial \tau^2}. \qquad (2)$$

As $b = 0$, we have the wave propagating with the group velocity dispersion β_2^0, which is set to one in the following. The corresponding Lagrangian density for Eq. (2) has the form

$$L = \frac{i(\bar{\psi}_\zeta \psi - \psi_\zeta \bar{\psi})}{2b|\psi|^2}\ln|-1 + b|\psi|^2| - \frac{1}{2}|\psi_\tau|^2. \qquad (3)$$

We note that Eq. (2) also preserves the U(1) symmetry, i.e., $\psi \to \exp[i\theta]\psi$. From the Noether theorem [9], one can obtain the conserved density for this model equation:

$$\frac{1}{b}\int_{-\infty}^{\infty}\ln|-1 + b|\psi|^2|d\tau. \qquad (4)$$

For $b = 0$, the corresponding Lagrangian density given in Eq. (3), as well as the conserved density given in Eq. (4), both go to infinity. In this limit, we only have plane wave solutions supported by linear dispersion.

To find soliton solutions with a confined spatial profile, we adopt the stationary ansatz

$$\psi = X(\tau)\exp[ic\zeta],$$

with the real function $X(\tau)$ to be determined for a given propagation constant $c > 0$. By substituting this ansatz into Eq. (2), one has

$$-cX(\tau) = [-1 + bX(\tau)^2]X''(\tau). \qquad (5)$$

By resorting to the concept of pseudo-potential [10,11], i.e., $X'' = -\nabla V(X)$, we can find the corresponding pseudo-potential for the intensity-dependent dispersion in Eq. (2), to be

$$V(X) = \int \frac{cX}{-1 + bX^2}dX = \frac{c}{2b}\ln|-1 + bX^2|, \qquad (6)$$

that vanishes at the origin, $V(X = 0) = 0$. The potential in Eq. (6) must be a trapping potential in order to support bright solitons as bound states. That is, the pseudo-potential must have either $b < 0$ to ensure that it is negative or $b > 0$ and $bX^2 < 2$.

In the latter case, the pseudo-potential has a singularity at $V(X) = 0$, for $X > 0$. The amplitude of the supported soliton is determined by $V(X) = 0$, so that $X = 2/b$. For these two cases, we can obtain the solution $X(\tau)$ from Eq. (5) with the asymptotic condition $X(\tau \to \infty) = 0$, by solving the Newtonian equation for a fictitious particle in the pseudo-potential, i.e., $\frac{1}{2}(\frac{dX}{d\tau})^2 = V(X)$:

$$|\tau - \tau_0| = \int_X^M \sqrt{\frac{-b}{c}} \frac{dX_1}{\sqrt{\ln(1 - bX_1^2)}}, \quad b < 0; \quad \textbf{(7)}$$

$$|\tau - \tau_0| = \int_X^M \frac{\sqrt{b}dX_1}{\sqrt{-c \ln|(-1 + bX_1^2)|}}, \quad b > 0. \quad \textbf{(8)}$$

Here, the maximum value X at τ_0 is assigned by $X(\tau_0) = M > 0$. In both cases, when $X \approx 0$, one can also apply Taylor's expansion for $\ln(1 - bX^2) \approx -bX^2 - b^2X^4/2 - b^3X^6/3 - \cdots$. Then, as $\sqrt{\frac{|b|}{|c|}} \frac{1}{\sqrt{\ln|-1+bX^2|}} \approx \sqrt{\frac{1}{|c|}} \frac{1}{X}$, we have $X \to 0$ as $\tau \to \pm\infty$. Due to the translation invariance, we can set $\tau_0 = 0$ for $X(0) = M$. Then, the corresponding derivative $X'(0)$ can be obtained as $X'(0) = -\sqrt{\frac{c}{b} \ln|-1 + bM^2|}$. Now, we can find soliton solutions for Eq. (7) or (8) with $b < 0$ or $b > 0$, respectively.

For a negative nonlinear coefficient, $b < 0$, one can match the asymptotics with the Taylor expansion near $\tau = 0$ and arrive at

$$|\tau| = -\ln(X)\frac{1}{\sqrt{c}} + \frac{1}{8}\frac{b}{\sqrt{c}}X^2 + O(X^4). \quad \textbf{(9)}$$

Then, we have the following approximation for the corresponding soliton solution:

$$X(\tau) \approx \exp\left[\frac{-1}{2}W\left(\frac{-1}{4}be^{-2\sqrt{c}|\tau|}\right) - \sqrt{c}|\tau|\right], \quad \textbf{(10)}$$

where W denotes the Lambert function defined as

$$W(z)e^{W(z)} = z.$$

Equation (10) is the main result of this work: it yields the soliton profile supported only by intensity-dependent dispersion. One can see that $X(\tau) \approx \exp[-\sqrt{-c}|\tau|]$ as $|\tau| \to \infty$ since $W(0) = 0$. It corresponds to the reduced linear equation in Eq. (2), i.e., $b = 0$. Moreover, as $|\tau| \to 0$, we have $X(0) = M = \exp[\frac{-1}{2}W(\frac{-1}{4}b)]$. Then, if $b \to -\infty$, we have $X(0) \to \infty$ as $\lim_{z\to\infty} W(z) \to \infty$.

A comparison between our analytical solution in Eq. (10) and a numerical solution obtained by directly solving Eq. (2) is depicted in Fig. 1. As shown by the solid curves, the soliton solution $X(\tau)$ derived in Eq. (10) almost perfectly matches the numerical ones obtained by directly solving Eq. (2). We also depict the corresponding pseudo-potential (dashed curve) as $V(\tau)$, by setting $b = 1$. Due to the reflection symmetry, the function $X(\tau)$ for $\tau < 0$ is constructed from Eq. (10) by taking $X(-\tau) = X(\tau)$. The maximum value of the soliton profile at $\tau = 0$ is set to be $X(\tau = 0) = M$. One can see that the derivative of the supported soliton profile diverges at the center,
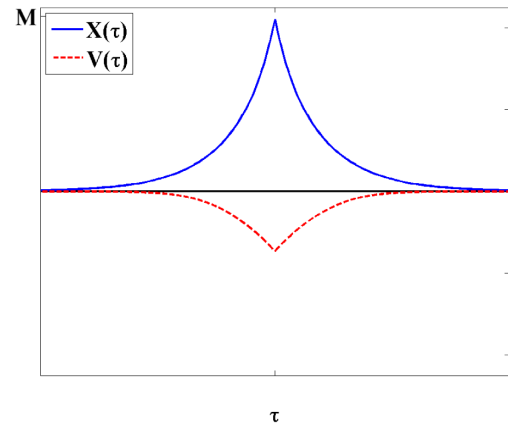
Fig. 1. Illustration of soliton solution $X(\tau)$ and its corresponding pseudo-potential $V(\tau)$, depicted in solid and dashed curves, respectively. The soliton is supported by intensity-dependent dispersion, with a negative value of the nonlinear coefficient $b = -1 < 0$. The soliton solution $X(\tau)$ derived in Eq. (10) almost perfectly matches the numerical one obtained by directly solving Eq. (2). Here, M denotes the maximum value of the soliton profile at $\tau = 0$, i.e., $X(\tau = 0) = M = 10^{12}$, and $c = 1$.

i.e., $dX(\tau = 0)/d\tau = \pm\infty$, which is known as the cuspons [12]. With the introduction of a non-zero nonlinear coefficient, the resulting pseudo-potential $V(\tau)$ acquires a discontinuity in its first-order derivative at $\tau = 0$.

The Lambert function $W(z)$ has the domain $z \in [-1/e, \infty)$, with the minimal value of -1 at $z = -1/e$. Hence, in Eq. (10), we have $-b \exp[-2\sqrt{c}\tau]/4 \geq -1/e$ or

$$\tau \geq \frac{|\ln|\frac{be}{4}||}{2\sqrt{c}} \approx \frac{\ln(b) - 0.3862}{2\sqrt{c}}. \quad \textbf{(11)}$$

This result approximates the soliton solution given in Eq. (10), as $|\tau| \to \infty$. In addition, when $-b \exp[-2\sqrt{c}x]/4 = -1/e$, one has the value

$$X(\tau_0) = \frac{|\ln|\frac{be}{4}||}{2\sqrt{c}}) \approx \sqrt{\frac{2}{b}}, \quad \textbf{(12)}$$

which is the maximum value for the amplitude of soliton solutions at τ_0.

Based on the above argument, we can set $M = \sqrt{2/b} > 0$ for a positive nonlinear coefficient, i.e., $b > 0$. In Fig. 2, we depict the numerical solutions for $X(\tau)$ by the solid curve, which is obtained by directly solving Eq. (2) with a positive value in the nonlinear coefficient, $b = +1$. Here, even-symmetry soliton solutions are constructed, i.e., $X(-\tau) = X(\tau)$. Except for the profile between the two points marked A and B, the tails of the soliton solution $X(\tau)$ can be almost exactly reconstructed from Eq. (10). As the corresponding pseudo-potential $V(\tau)$ goes to ∞ at points A and B (see the dashed curve), the derivatives of the supported soliton profile also diverge at these two points.

Even though the supported soliton solution shown in Fig. 2 has points with divergent derivatives at the corresponding pseudo-potential, one can prove that the corresponding conserved density still remains finite, and thus the solution is physical. By using the relation between τ and X given in Eq. (8), one can change the integral variable in Eq. (4),
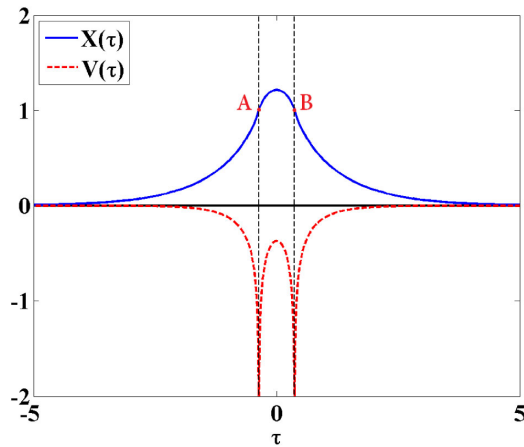
Fig. 2. One-humped soliton solution $X(\tau)$ and the corresponding pseudo-potential $V(\tau)$, depicted by solid and dashed curves, respectively, for a positive value of the nonlinear coefficient $b = +1 > 0$. The tails of the soliton solution $X(\tau)$ obtained numerically from Eq. (2) can be reconstructed from Eq. (10). The corresponding pseudo-potential is divergent at the two points marked A and B, where $dV/d\tau = \pm\infty$ and $c = 1$.
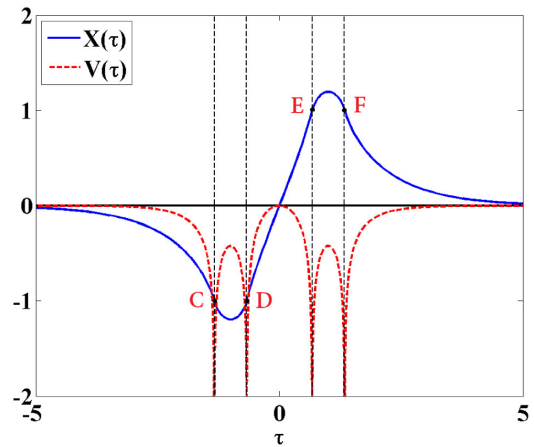

Fig. 3. Two-humped soliton solution $X(\tau)$ and its corresponding pseudo-potential $V(\tau)$, depicted by solid and dashed curves, respectively, for a positive value of the nonlinear coefficient $b = +1 > 0$. Here, the corresponding pseudo-potential is divergent at the points marked C, D, E, and F, where $dV/d\tau = \pm\infty$.

$$\frac{1}{\sqrt{bc}} \int_0^M \sqrt{\ln|-1 + bX_1^2|}\,dX_1$$

$$= \frac{1}{\sqrt{bc}} \left[\int_0^{\frac{1}{\sqrt{b}}} \sqrt{\ln(1 - bX_1^2)}\,dX_1 + \int_{\frac{1}{\sqrt{b}}}^M \sqrt{\ln(-1 + bX_1^2)}\,dX_1 \right]$$

$$= \frac{1}{2b} \left[\int_0^1 \frac{\sqrt{\frac{\ln u}{c}}}{\sqrt{1 - u}}\,du + \int_0^{bM^2 - 1} \frac{\sqrt{\frac{\ln u_1}{c}}}{\sqrt{1 + u_1}}\,du_1 \right], \tag{13}$$

where we have introduced $u \equiv 1 - bX_1^2$ and $u_1 \equiv -1 + bX_1^2$. As it is known that $\lim_{u \to 1^-} \frac{\ln u}{1 - u} = -1$ by the *L'hopital* rule, the convergence of improper integrals in Eq. (13) depends on the integral $\int_0^\alpha \sqrt{\frac{\ln v}{c}}\,dv$ for a finite positive α near $v = 0$. By choosing $\alpha = 1$ for the scaling, we have
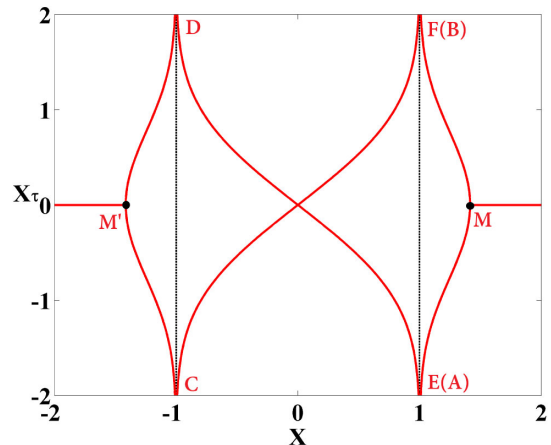
$$\int_0^1 \sqrt{\frac{\ln v}{c}}\,dv = \sqrt{\frac{-1}{c}} \int_0^\infty y^{1/2} e^{-y}\,dy$$

$$= \sqrt{\frac{-1}{c}}\, \Gamma(3/2) = \sqrt{\frac{-\pi}{4c}},$$

with $v = e^{-y}$. Hence, the conserved density of our stationary soliton solution is convergent even for a nonlinear dispersion coefficient $b > 0$.

In addition to the one-humped even-symmetry soliton solutions displayed in Fig. 2, we can also construct odd-symmetry two-humped soliton solutions for a positive value of the nonlinear coefficient $b = +1$. One can see in Fig. 3 the odd-symmetry soliton solution $X(\tau)$ depicted by a solid curve, i.e., $X(-\tau) = -X(\tau)$, upon setting $M = 0$. The corresponding potential $V(\tau)$, depicted by a dashed curve, has four singular values at the points marked C, D, E, and F. We can check from Eq. (2) that a finite value of the conserved density exists for the two-humped soliton solution.


Fig. 4. Phase diagram defined by X and $X_\tau \equiv dX/d\tau$ for our soliton solutions. Here, the sets of points marked (A, B) and (C, D, E, F) correspond to the marked points in Figs. 2 and 3, respectively, while the points M and M′ give the maximum value of the soliton profile. As $b = +1$ is chosen, we have $X = \pm 1/\sqrt{b} = \pm 1$ for the amplitudes in the soliton profile, at which the derivative goes to $\pm\infty$.

An alternative picture that provides deeper understanding of our soliton solutions is obtained from the phase diagram for the Newtonian pseudo-particle dynamics, defined by X and $X_\tau \equiv dX/d\tau$. For the one-humped solution, one may follow the trajectory on the right-hand side of this phase diagram, where $X \geq 0$ (Fig. 4). By starting at the origin $(X, X_\tau) = (0, 0)$ and following the trajectory to the point marked B $(1/\sqrt{b} = 1, \infty)$, we find an infinite derivative of the profile. The soliton profile goes through its maximum value (the point marked M) to its other infinite derivative (point marked A) and finally back to the origin $(0,0)$. This trajectory exactly reflects the one-humped soliton solution illustrated in Fig. 2. By following the two sides of the trajectory in Fig. 4, $X \geq 0$ and $X \leq 0$, one can easily construct the two-humped soliton solutions illustrated in Fig. 3.
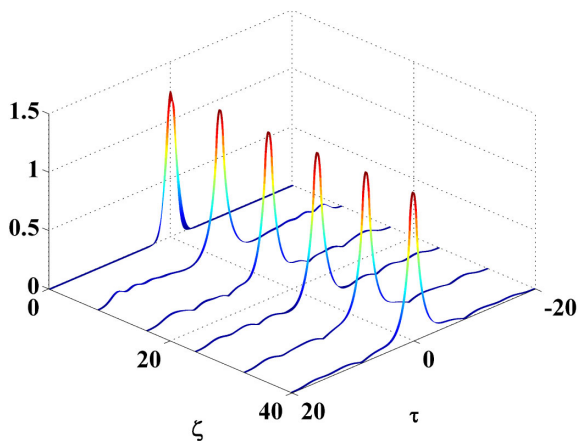
Fig. 5. Evolution for an initial Gaussian profile applied to Eq. (2) directly. Within the propagation distance up to $\zeta = 40$, the resulted profile resembles our finding of an analytic solution.

In conclusion, our analysis reveals the existence of singularities in the pseudo-potential associated with intensity-dependent dispersion, resulting in one- and two-humped supported solitons with infinite derivatives in their profiles. The tails of these solitons can be described by Lambert functions, which give almost perfect agreement to the numerical solutions of the paraxial wave equation with intensity-dependent dispersion. Even though such discontinuities in the derivative of soliton profiles make them unstable (as we have checked by linear stability analysis and by the Vakhitov–Kolokolov stability criterion), their conserved density still remain finite, attesting to the physicality of the solutions. By using an initial Gaussian profile applied to Eq. (2) directly, we illustrate in Fig. 5 the evolution of this approximated solution through numerical simulation. Within a certain propagation distance (up to $\zeta = 40$ here), the resulted profile resembles our finding of the analytic solution.

As nonlinear corrections to the dispersion arise in a variety of wave phenomena, our results may open a hitherto unexplored area of nonlinear wave propagation. Through the correspondence between the paraxial wave equation and the Schrödinger equation (upon replacing $\zeta \to t$ and $\tau \to x$), our model equation can also be applied to a quantum particle (electron or hole) with a nonlinear effective mass $m^*(|\psi|^2)$, i.e., $i\hbar\psi_t = [1/2m^*(|\psi|^2)]\psi_{xx}$. In a non-uniform potential, a quantum particle may acquire an intensity-dependent effective mass. For example, in nonlinear photonic crystals, strong coupling between nonlinearity and diffraction at the super-collimation point can be modeled with a nonlinear diffraction term [13]. Such a scenario has gained much interest in view of its applications, ranging from semiconductors to quantum fluids [14–20].

A number of promising applications and directions for further exploration may be identified: (a) the present soliton model may be connected to off-resonant electromagnetic (EM) propagation in two-level media outside the domain of resonant self-induced transparency (SIT) solitons [21,22]. (b) In media with spatially periodic refractivity doped with two-level systems (TLS), the spatial modulation of the propagating EM intensity may enhance the intensity-dependent nonlinear TLS dispersion [23,24]. (c) In the EIT regime of three-level atoms that are coupled via resonant dipole–dipole interactions, the present soliton solutions may be related to the previously explored long-range photon–photon interactions [25,26]. (d) The nonlinear effective mass appears in the continuum limit of the Salerno model, which originally describes a quantum-modified discrete nonlinear Schrödinger equation with on-site focusing and defocusing inter-site nonlinearities [27].

Disclosures. The authors declare no conflicts of interest.

REFERENCES

1. G. P. Agrawal, *Nonlinear Fiber Optics*, 4th ed. (Academic, 2007).
2. G. B. Whitham, J. Fluid Mech. **22**, 2733 (1965).
3. G. B. Whitham, *Linear and Nonlinear Waves* (Wiley, 1999).
4. V. E. Gusev, W. Lauriks, and J. Thoen, J. Acoust. Soc. Am. **103**, 3216 (1998).
5. A. A. Koser, P. K. Sen, and P. Sen, J. Mod. Opt. **56**, 1812 (2009).
6. A. Javan and A. Kelley, IEEE J. Quantum Electron. **2**, 470 (1966).
7. A. D. Greentree, D. Richards, J. A. Vaccaro, A. V. Durrant, S. R. de Echaniz, D. M. Segal, and J. P. Marangos, Phys. Rev. A **67**, 023818 (2003).
8. E. Shahmoon, P. Grisins, H. P. Stimming, I. Mazets, and G. Kurizki, Optica **3**, 725 (2016).
9. P. J. Olver, *Applications of Lie Groups to Differential Equations*, 2nd ed. (Springer Verlag, 1993).
10. M. J. Ablowitz and H. Segur, *Solitons and the Inverse Scattering Transform* (SIAM, 1981).
11. R. C. Davidson, *Methods in Nonlinear Plasma Theory* (Academic, 1972).
12. H. Sakaguchi and B. A. Malomed, Phys. Rev. A **83**, 013607 (2011).
13. Z. Xu, B. Maes, X. Jiang, J. D. Joannopoulos, L. Torner, and M. Soljačić, Opt. Lett. **33**, 1762 (2008).
14. O. von Roos, Phys. Rev. B **27**, 7547 (1983).
15. A. de Souza Dutra and C. A. S. Almeidab, Phys. Lett. A **275**, 25 (2000).
16. A. G. M. Schmidt, Phys. Lett. A **353**, 459 (2006).
17. P. K. Jha, H. Eleuch, and Yu. V. Rostovtsev, J. Mod. Opt. **58**, 652 (2011).
18. R. N. Costa Filho, M. P. Almeida, G. A. Farias, and J. S. Andrade, Jr., Phys. Rev. A **84**, 050102 (2011).
19. M. Sebawe Abdalla and H. Eleuch, AIP Adv. **6**, 055011 (2016).
20. J. H. Chang, C.-Y. Lin, and R.-K. Lee, "Nonlinear effective mass Schrödinger equation with harmonic oscillator," arXiv: 1911.12477 (2019).
21. A. I. Maimistov, A. M. Basharov, S. O. Elyutin, and Yu. M. Sklyarov, Phys. Rep. **191**, 1 (1990).
22. M. Blaauboer, B. A. Malomed, and G. Kurizki, Phys. Rev. Lett. **84**, 1906 (2000).
23. A. Kozhekin and G. Kurizki, Phys. Rev. Lett. **74**, 5020 (1995).
24. A. E. Kozhekin, G. Kurizki, and B. Malomed, Phys. Rev. Lett. **81**, 3647 (1998).
25. I. Friedler, D. Petrosyan, M. Fleischhauer, and G. Kurizki, Phys. Rev. A **72**, 043803 (2005).
26. E. Shahmoon, G. Kurizki, M. Fleischhauer, and D. Petrosyan, Phys. Rev. A **83**, 033806 (2011).
27. M. Marklund, P. K. Shukla, R. Bingham, and J. T. Mendonca, Phys. Rev. A **74**, 045801 (2006).